Nanoscale

Accepted Manuscript

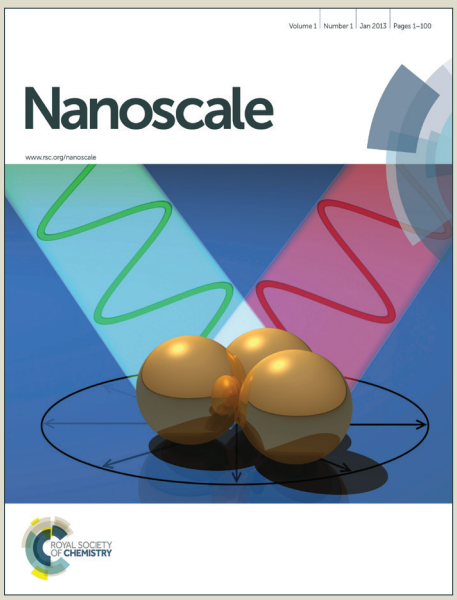

ROYAL SOCIETY OF CHEMISTRY

www.rsc.org/nanoscale

Journal Name

ARTICLE

Understanding and optimising the packing density of perylene bisimide layers on CVD-grown graphene

Received 00th January 20xx,
Accepted 00th January 20xx

DOI: 10.1039/x0xx00000x

www.rsc.org/

Nina C. Berner[a], Sinéad Winters[a,b], Claudia Backes[c], Chanyoung Yim[a,b], Kim C. Dümbgen[a], Izabela Kaminska[d], Sebastian Mackowski[d], Attilio A. Cafolla[e], Andreas Hirsch[f], and Georg S. Duesberg[a,b]

The non-covalent functionalisation of graphene is an attractive strategy to alter the surface chemistry of graphene without damaging its superior electrical and mechanical properties. Using the facile method of aqueous-phase functionalisation on large-scale CVD-grown graphene, we investigated the formation of different packing densities in self-assembled monolayers (SAMs) of perylene bisimide derivatives and related this to the amount of substrate contamination. We were able to directly observe wet-chemically deposited SAMs in scanning tunnelling microscopy (STM) on transferred CVD graphene and revealed that the densely packed perylene ad-layers adsorb with the conjugated π-system of the core perpendicular to the graphene substrate. This elucidation of the non-covalent functionalisation of graphene has major implications on controlling its surface chemistry and opens new pathways for adaptable functionalisation in ambient conditions and on the large scale.

Introduction

Since the isolation of single layer graphene by mechanical exfoliation[1] and the subsequent discovery and demonstration of its outstanding electronic[2] and mechanical[3] properties, graphene has attracted an extremely high level of interest. It has been proposed for numerous applications in electronics,[4] photonics,[5, 6] sensing,[7] as well as gas barriers[8] and coatings.[9] However, for most of these applications it is necessary to introduce functional groups onto the graphene surface, *e.g.* to achieve sensor selectivity.

Non-covalent functionalisation is an attractive strategy to introduce chemical functionalities since it does not adversely affect the electronic properties of the graphene layer.[10-12] Organic molecules with a relatively large and planar aromatic core have been repeatedly reported, both experimentally and theoretically, to adsorb on the graphene surface *via* van der Waals interactions between the extended π-orbital systems of the molecular core and the graphene, often referred to as π-π stacking.[13-15] Most detailed studies on the non-covalent functionalisation of graphene have been conducted on either chemically exfoliated graphene flakes in solution[16] or on epitaxially grown graphene on SiC substrates in ultra-high vacuum (UHV).[17, 18] However, neither of these graphene preparation methods is suitable for the fabrication of devices on an industrial scale. Graphene grown by chemical vapour deposition (CVD) is better suited for industrial electronic applications, especially since the growth and transfer onto SiO_2 substrates have been vastly improved in recent years[19, 20] and CVD can now produce graphene of high structural integrity and with electrical characteristics that can compete with those of mechanically exfoliated graphene.[21, 22]

Non-covalent functionalisation of CVD graphene can be achieved by thermal evaporation[23, 24] or by deposition of the molecules from liquid phase.[25-27] However, a few recent studies have shown that the mode of deposition[28] and the nature of the graphene substrate[29] have a significant influence on the adsorption geometry and molecular orientation in the ad-layers, which is a very important factor since it has been shown to influence the film's characteristics such as light adsorption, charge transport and energy level alignment[30]. These findings imply that many of the reported results obtained on *e.g.* epitaxially grown graphene and with molecules evaporated under UHV conditions may not be applicable to the same or very similar material systems obtained by scalable methods like CVD growth and subsequent wet-chemical functionalisation. Nevertheless, investigating the

[a] *Centre for the Research on Adaptive Nanostructures and Nanodevices (CRANN) and Advanced Materials and BioEngineering Research (AMBER), Trinity College Dublin, Dublin 2, Ireland*
[b] *School of Chemistry, Trinity College Dublin, Dublin 2, Ireland*
[c] *School of Physics, Trinity College Dublin, Dublin 2, Ireland*
[d] *Faculty of Physics, Astronomy and Informatics, Nicolaus Copernicus University, Grudziadzka 5, 87-100 Torun, Poland*
[e] *School of Physical Sciences, Dublin City University, Dublin 13, Ireland*
[f] *Institute of Organic Chemistry II, University of Erlangen-Nürnberg, Henkestr. 42, 91054 Erlangen, Germany*

Electronic Supplementary Information (ESI) available: Additional Raman spectra of the graphene substrates before and after annealing and deposition of **1**, fluorescence images of multilayer regions of **1**, a more detailed discussion of SE results, and some additional STM images can be found in the Supporting Information (SI). See DOI: 10.1039/x0xx00000x

thus obtained material systems is challenging for a number of reasons. It has been demonstrated that electrical measurements obtained from wet-chemically deposited molecule films on graphene can be difficult to reproduce due to unwanted and uncontrollable doping and disturbance of the structural uniformity of the molecular layers by solvent co-adsorption.[26, 27] In addition, the presence of transfer polymer residue on CVD graphene has been shown to affect the organisation of the molecular layers.[29, 31] These effects can be significantly reduced by optimising the quality of the graphene surface. Here we describe the functionalisation of graphene with a water-soluble perylene bisimide derivative **1**, shown in Figure 1a, from the liquid phase and its characterisation with water contact angle measurements, Raman and fluorescence spectroscopy, spectroscopic ellipsometry (SE) as well as, for the first time at room temperature, STM with atomic resolution of an organic ad-layer directly on transferred CVD graphene in UHV.

Molecules similar to **1** have previously been used as surfactants in liquid exfoliation of carbon allotropes.[16, 32, 33] It was assumed that the aromatic perylene core is adsorbed on the carbon allotrope *via* π-π stacking, while the carboxylic acid groups terminating the dendritic side chains stabilise the dispersed carbon allotropes in water. However, such molecular systems are also of great interest in terms of non-covalent functionalisation of CVD graphene, as the carboxylic acid groups are highly potent anchor groups for further derivatisation. It is therefore important to understand and tune the adsorption behaviour. In this study, we demonstrate the influence of the cleanliness of the graphene surface on the packing density of the films and investigate the geometry of the most densely packed self-assembled monolayers.

Experimental

Raman spectroscopy

Raman studies were conducted in air, using a WiTec Alpha 300 nm confocal Raman system with a 532 nm excitation laser wavelength. Raman maps were acquired with a point spectrum taken every 400 nm and an integration time of 0.1 s/spectrum. The intensity of all spectra was normalised to the intensity of the graphene G peak before further processing, *i.e.* the calculation of intensity ratios and the mapping thereof. All analysis was done using the WiTec Project software.

Scanning Tunnelling Microscopy

Scanning Tunnelling Microscopy (STM) measurements were performed in UHV (pressure < 10^{-10} mbar) at room temperature on an Omicron Variable Temperature (VT)-STM. Samples were attached to tantalum sample plates using tantalum wire, which also helped to ensure electrical contact between the graphene film and the sample plate. The STM tips used in these experiments were electrochemically etched from tungsten wire (0.15 mm diameter) using 2M KOH. The imaging parameters used for each image displayed in this manuscript are provided individually with every figure. The images underwent minimal processing steps limited to FFT-supported flattening and Gaussian blurs (over 2px) using the software WSxM.[34]

Spectroscopic Ellipsometry

An Alpha SE tool (J. A. Woollam Co., Inc.) was used for the Spectroscopic Ellipsometry (SE) data measurements, operating in the wavelength range of 380 – 900 nm (1.38 – 3.25 eV) at an angle of incidence of 65° with a beam spot size of ~40 mm^2. The measured data was analysed using the CompleteEASE software (Ver.4.72, J. A. Woollam Co., Inc.). The SE system gathered values of psi (Ψ) and delta (Δ), which represent the amplitude ratio (Ψ) and phase difference (Δ) between p- and s-polarizations, over the specific wavelength range. The two parameters are related to the ratio ρ, defined by the equation of $\rho = r_p/r_s = \tan(\Psi)\exp(i\Delta)$, where r_p and r_s are the amplitude reflection coefficients for the p-polarized and s-polarized light, respectively.

Fluorescence microscopy and lifetime measurements

Spectrally- and time-resolved fluorescence measurements were performed using a home-built confocal fluorescence microscope described in detail elsewhere.[35] The sample was placed on a piezoelectric translation stage, which enabled continuous movement of the sample with respect to the excitation laser beam. We used pulsed laser excitation at 485 nm (with a repetition rate of 20 MHz and power of 10 µW). Fluorescence was extracted using a combination of FEL550 + 665/40 filters.

Wide-field microscopy imaging experiments of the perylene on graphene samples were carried out using an inverted fluorescence wide-field Nikon Eclipse Ti-U microscope equipped with an Andor iXon Du-888 EMCCD detector. Immersion objective with magnification 100x (Plan Apo, Nikon) and the numerical aperture 1.4 was used, which provides spatial resolution of about 300 nm. As a light source we used an LED illuminator (485 nm) equipped with a band pass filter (FB 480-10). Excitation power was equal to 100 µW. Fluorescence of **1** on graphene was extracted by combining a dichroic mirror (Chroma 505dcxr) and a band pass filter (Thorlabs FB 655-40).

Materials

Graphene was grown on copper foil by CVD, using methane as the carbon source at a temperature of 1035°C, as described in more detail previously.[19] Sample-sized pieces (typically around 1 x 1 cm^2) were subsequently transferred on a Si/SiO_2 (300 nm or 150 nm) substrate using the established PMMA-assisted method. In a typical process, a 100 nm film of PMMA was spun-cast on the graphene grown on the copper substrate. The copper was subsequently etched in a 1M ammonium persulfate solution. The remaining PMMA/graphene layer was floated onto de-ionized water and left to rinse for 1 hour. The film was then transferred to the substrates and left to dry in air. The PMMA was removed by

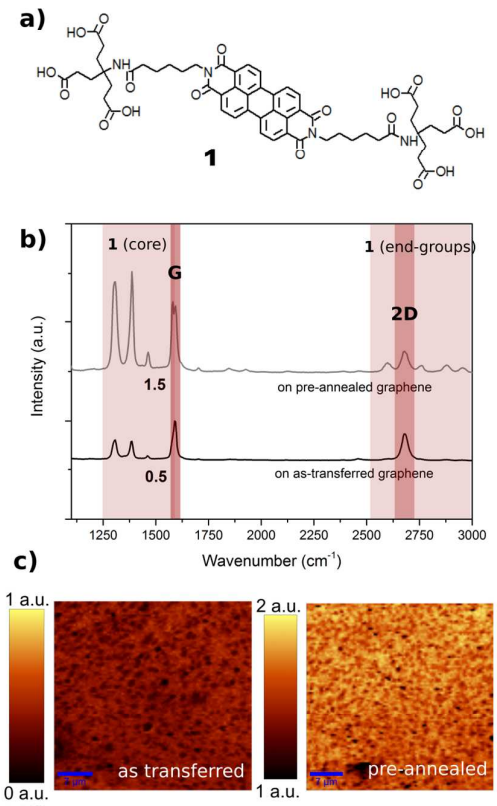

Figure 1. a) Chemical structure of Perylene **1**, b) average Raman spectra of **1** deposited on as-transferred and annealed CVD-grown graphene on SiO_2, with peak assignment labels for colored wavenumber regions, c) corresponding Raman maps of **1** (core):G peak ratio in LPD and HPD layers.

immersion in acetone overnight. To produce annealed samples with reduced PMMA residue, substrates were annealed overnight in UHV (pressure < 10^{-9} mbar) at a temperature of 220°C.

Perylene **1** was synthesised as described elsewhere[36] and then dissolved in aqueous sodium phosphate buffer solution (pH 7, 0.1M) at a concentration of 0.001 mol L^{-1}. No other solvents were used in this study, which is briefly discussed in the SI. The solution was applied to the graphene surface by drop-casting or dip-casting for 5-10 seconds and subsequent rinsing with de-ionised water and isopropyl alcohol. The samples were blow-dried with dry nitrogen before characterisation. Different perylene concentrations and deposition times were found to have negligible effects on the layer formation, as briefly discussed in the SI.

Results and Discussion

After the deposition of **1** onto CVD-grown graphene from aqueous solution, as described in detail in the Experimental section, the layers were investigated with Raman spectroscopy. The perylene molecules can be easily identified

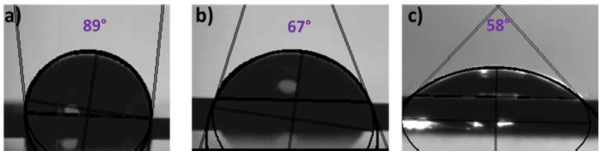

Figure 2. Water contact angle measurements of a) clean graphene, b) low packing density **1** layer on graphene, and c) high packing density **1** layer on graphene.

and characterised by their two major characteristic Raman peaks at 1303 cm^{-1} and 1383 cm^{-1} when resonantly excited at 532 nm, as previously described and demonstrated by Kozhemyakina *et al.* on liquid-exfoliated graphene.[37] The ratio of those two most intense **1** peaks to the G peak of the graphene substrate (**1**:G) can be seen as an indicator of the packing density of the molecular layer. The black curve in Figure 1b shows a Raman spectrum of **1** deposited on CVD-grown graphene after it was transferred onto SiO_2 using a standard PMMA-assisted process as described in detail elsewhere.[19] Figure 1c shows the corresponding Raman intensity maps of the **1**:G intensity ratio over a 30 x 30 μm^2 area, showing very high uniformity except in small patches which correspond to 2nd layer graphene growth. The **1**:G peak ratio was determined to be 0.5 on average. With very high reproducibility, the packing densities of the molecular films are much higher when **1** was deposited on a transferred graphene substrate which had been previously annealed to reduce PMMA residue,[38] as can be seen in the grey spectrum in Fig. 1b and the **1**:G ratio map in Figure 1c. We attribute this to the absence of polymer or other hydrocarbon contaminants on the pre-annealed graphene surface, which allows the perylene molecules to rearrange more easily and to self-assemble into a densely packed layer. Further details of additional peaks in the Raman spectrum of **1** are provided in the SI.

The different packing densities of **1** on graphene also have an effect on the layer thickness as estimated by spectroscopic ellipsometry (SE). From a model that is discussed in detail in the SI, the **1** layers on as-transferred and pre-annealed graphene substrates were measured to be 2.2 (± 0.1) nm and 5.4 (± 0.2) nm thick, corresponding to the low (LPD) and high packing density (HPD), respectively. The difference between these values underlines the significance of the packing density variation.

The significantly increased packing density of **1** on cleaner graphene is further confirmed by water contact angle (WCA) measurements, typical examples of which are depicted in Figure 2. Bare graphene samples on SiO_2 have a water contact angle of 89° (±1°), similar to what has been reported elsewhere.[39] The contact angle is decreased upon addition of **1** to the surface, due to the presence of hydrophilic groups, in particular the six carboxylic acid functions. For graphene samples with LPD perylene molecules, a water contact angle of 67° (±2°) is measured, while an angle of 58° (±2°) is observed at HPD layers of **1**, clearly indicating an increase in the number of carboxylic acid groups on the surface.

The exact nature of the HPD layers is further investigated by characterisation of the transferred graphene substrate and subsequent perylene **1** deposition by scanning tunnelling microscopy (STM). Figure 3a shows an STM image of CVD-grown graphene transferred with PMMA on SiO_2 before and after an overnight anneal in UHV at 220°C. As clearly visible in the upper part of Figure 3a, images taken on the as-transferred surface show streaky features that indicate loosely bound material which is moved over the surface by the STM tip. In contrast, images taken on the same surface after the overnight anneal are much clearer and show almost no evidence of adsorbates. After deposition of **1** on the pre-annealed, clean graphene substrate and a short anneal to just over 100°C to remove any adsorbed water, STM images taken over the entire surface area show periodic structures as shown in Figure 3b, which, upon closer inspection, can be related to molecular arrays. Figure 3c shows line profiles across some of the features which reveal periodicities of 0.23 nm and 3.25 nm along orthogonal directions (further images and analysis are shown in the SI). This leads us to the conclusion that in its HPD configuration, **1** adsorbs and packs into SAMs with the perylene cores perpendicular to the surface, as indicated by the molecular structure overlay in Figure 3d and visualised in Figure S4e. This observation is in contrast to the common assumption that organic molecules with large conjugated π-systems adsorb via π-π interactions between the molecular cores and the graphene substrate, regardless of the method of deposition and preparation method of the graphene. Our findings emphasize that the adsorption of molecules on surfaces is governed by a complex interplay of interfacial energies between both the molecules themselves and the molecules and the substrate's surface. If molecules are deposited from solution, they are surrounded by a much larger number of neighbouring molecules than if they were deposited by thermal evaporation, which changes the energy landscape and therefore the adsorption behaviour significantly. This is particularly the case for **1** which is not present as monomer in solution, but forms micelles due to the strong interaction between the perylene cores and the amphiphilic nature of the molecules.[36] The other major influencing factor is the surface energy of the substrate, which is evidenced by the difference in adsorption behaviour of **1** when the graphene substrate is contaminated with PMMA residue. In the particular case of the HPD layer of **1** on clean CVD graphene, it appears that the molecule-molecule interactions are much stronger than the molecule-substrate interactions, but this may be different in an even slightly altered environment, for example by residual PMMA on the substrate. This is indirectly supported by STM images recorded on samples with LPD of **1**, an example of which is shown in Figure S4f. None of the images showed any clearly resolved features, which indicates an abundance of loose material on the surface and the lack of molecule-molecule stabilisation in organised structures. Previous studies on varying coverages of 6P molecules on graphene show that the adsorption geometry and orientation of organic molecules with aromatic π-systems can be strongly coverage dependent.[40] Therefore the adsorption geometry is likely to be different for LPD perylene films. In fact, the lower density of carboxylic acid groups evidenced by the WCA measurements implies that at least some of the molecules are adsorbed with the perylene core lying flat on the substrate.

However, the results of fluorescence imaging and spectroscopy also provide some evidence of vertical packing of **1** on graphene in the LPD structure. Figure 4a shows an example of a fluorescence image obtained for a 100 x 90 μm^2 area. While the intensity is rather low and some completely dark areas are visible, a large fraction of the sample exhibits measurable emission. The overall low emission intensity is a result of both monolayer coverage of **1** on the graphene substrate and energy transfer to graphene. Spectrally-resolved and time-resolved data (Figures 4b and c), obtained for fluorescent regions on the sample shows that the emission of **1** appears around 670 nm, which is dramatically shifted to longer wavelengths as compared to the solution.[41] This points towards a strong interaction between the aromatic rings of the molecules, which is possible only in a configuration where the molecules are placed at an angle to the substrate. Furthermore, a much shorter fluorescence decay evidences an energy transfer with a low efficiency of less than 80%, which again suggests that not all of the molecules are lying flat on the surface, as this would promote essentially complete quenching of the fluorescence.[42] The observations obtained for the LPD structure are corroborated with the results of analogous experiments for regions with multilayer coverage, where several-layer-thick regions are present in addition to

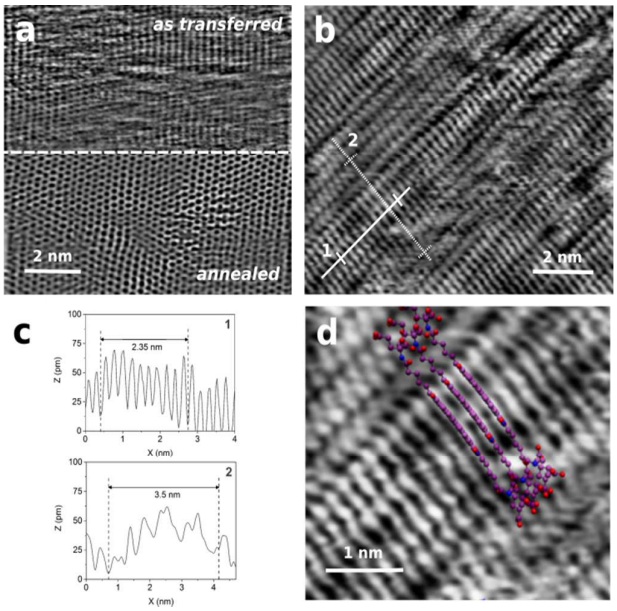

Figure 3. STM images of a) as-transferred (top, taken at -0.3 V/0.3 nA) and subsequently annealed (bottom, taken at -0.5 V/0.8 nA) CVD graphene on SiO_2 and b) after wet-chemical deposition of **1** on the same annealed substrate (taken at -0.5 V/0.1 nA); c) line profiles from b) and zoomed in area with molecular structure overlay (d).

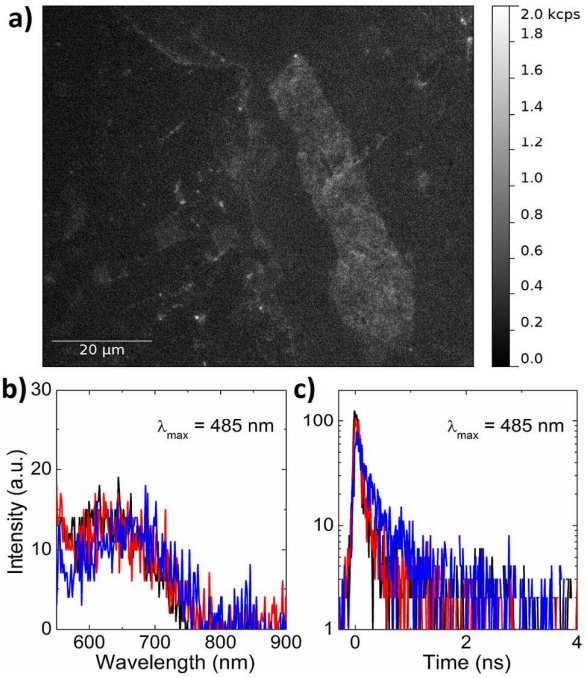

Figure 4. a) Wide-field fluorescence image of LPD **1** on graphene. b) Typical fluorescence spectra and c) fluorescence decay curves obtained for three different locations across the LPD sample. Excitation at 485 nm was used in both experiments.

monolayer areas (see SI). In particular, the spectral position of high-intensity regions is exactly the same as for monolayer regions, which further supports that the molecular orientation vertical to the graphene substrate is the most energetically favorable and that molecule-molecule interactions within the same self-assembled layer are the dominating factor, even in multilayers.

Conclusions

In summary, we report on the non-covalent functionalisation of CVD-grown and transferred graphene from aqueous solution. We demonstrated the dependency of the packing density of perylene bisimide derivative ad-layers on the surface contamination of the graphene substrate, as easily recognisable from Raman spectroscopy, SE and WCA measurements. Furthermore, fluorescence spectroscopy and STM images of densely packed perylene films on CVD graphene reveal a vertical adsorption geometry stabilised by π-π interactions between the cores of the molecules. The altered surface energy of the graphene caused by transfer polymer residue appears to alter the adsorption geometry of the perylenes and cause them to adsorb with the core flat or at least at a lower angle to the substrate in some regions, while still standing upright in others. This increased understanding of the adsorption and self-assembly of wet-chemically deposited organic molecules on CVD-grown and transferred graphene highlights the often underestimated complexity of molecular adsorption on graphene and is therefore an important step towards the reliable large-scale fabrication of non-covalently functionalised 2D materials and their application.

Acknowledgements

NCB, SW and GSD acknowledge the SFI under grant number PI_10/IN.1/I3030. The research leading to these results has also received funding from the European Union Seventh Framework Program under grant agreement n°604391 Graphene Flagship. In addition, CB acknowledges the German research foundation DFG (BA 4856/1-1). IK and SM are supported by the project number DEC-2013/10/E/ST3/00034 from the National Science Center (NCN). AH would like to thank the DFG (SFB 953 Synthetic Carbon Allotropes) for financial support. AAC thanks the SFI, grant number 08/RFP/PHY1366. We thank Christian Wirtz for providing the schematics.

References

1 K. S. G. Novoselov, A. K.; Morozov, S. V.; Jiang, D.; Zhang, Y.; Dubonos, S. V.; Grigorieva, I. V.; Firsov, A. A., *Science*, 2004, **306**, 666-669.

2 R. V. G. A.S. Mayorov, S.V. Morozov, L. Britnell, R. Jalil, L.A. Ponomarenko, P. Blake, K.S. Novoselov, K. Watanabe, T. and A. K. G. Taniguchi, *Nano Letters*, 2011, **11**, 2396-2399.

3 C. Lee, X. Wei, J. W. Kysar and J. Hone, *Science*, 2008, **321**, 385-388.

4 F. Xia, D. B. Farmer, Y.-m. Lin and P. Avouris, *Nano Letters*, 2010, **10**, 715-718.

5 J. Wu, M. Agrawal, H. A. Becerril, Z. Bao, Z. Liu, Y. Chen and P. Peumans, *ACS Nano*, 2009, **4**, 43-48.

6 Z. Liu, Q. Liu, Y. Huang, Y. Ma, S. Yin, X. Zhang, W. Sun and Y. Chen, *Advanced Materials*, 2008, **20**, 3924-3930.

7 X. D. Yuxin Liu, Peng Chen, *Chemical Society Reviews*, 2012, **41**, 2283–2307.

8 J. S. Bunch, S. S. Verbridge, J. S. Alden, A. M. van der Zande, J. M. Parpia, H. G. Craighead and P. L. McEuen, *Nano Letters*, 2008, **8**, 2458-2462.

9 D. Prasai, J. C. Tuberquia, R. R. Harl, G. K. Jennings and K. I. Bolotin, *ACS Nano*, 2012, **6**, 1102-1108.

10 V. O. Georgakilas, M.; Bourlinos, A. B.; Chandra, V.; and N. K. Kim, K. C.; Hobza, P.; Zboril, R.; Kim, K. S., *Chemical Reviews*, 2012, **112**, 6156−6214.

11 J. A. Mann and W. R. Dichtel, *The Journal of Physical Chemistry Letters*, 2013, **4**, 2649-2657.

12 H. Y. Mao, Y. H. Lu, J. D. Lin, S. Zhong, A. T. S. Wee and W. Chen, *Progress in Surface Science*, 2013, **88**, 132-159.

13 J. Björk, F. Hanke, C.-A. Palma, P. Samori, M. Cecchini and M. Persson, *The Journal of Physical Chemistry Letters*, 2010, **1**, 3407-3412.

14 A. J. Pollard, E. W. Perkins, N. A. Smith, A. Saywell, G. Goretzki, A. G. Phillips, S. P. Argent, H. Sachdev, F.

Müller, S. Hüfner, S. Gsell, M. Fischer, M. Schreck, J. Osterwalder, T. Greber, S. Berner, N. R. Champness and P. H. Beton, *Angewandte Chemie International Edition*, 2010, **49**, 1794-1799.
15 H. H. Zengxing Zhang, Xiaomei Yang, Ling Zang, *Journal of Physical Chemistry Letters*, 2011, **2**, 2897-2905.
16 C. Backes, F. Hauke and A. Hirsch, *Advanced Materials*, 2011, **23**, 2588-2601.
17 Q. H. Wang and M. C. Hersam, *Nat Chem*, 2009, **1**, 206-211.
18 H. Huang, S. Chen, X. Gao, W. Chen and A. T. S. Wee, *ACS Nano*, 2009, **3**, 3431-3436.
19 T. Hallam, N. C. Berner, C. Yim and G. S. Duesberg, *Advanced Materials Interfaces*, 2014, **1**, 1400115.
20 C. Wirtz, K. Lee, T. Hallam and G. S. Duesberg, *Chemical Physics Letters*, 2014, **595–596**, 192-196.
21 N. Petrone, C. R. Dean, I. Meric, A. M. van der Zande, P. Y. Huang, L. Wang, D. Muller, K. L. Shepard and J. Hone, *Nano Letters*, 2012, **12**, 2751-2756.
22 S. Hurch, H. Nolan, T. Hallam, N. C. Berner, N. McEvoy and G. S. Duesberg, *Carbon*, 2014, **71**, 332-337.
23 Y. Ogawa, T. Niu, S. L. Wong, M. Tsuji, A. T. S. Wee, W. Chen and H. Ago, *The Journal of Physical Chemistry C*, 2013, **117**, 21849-21855.
24 H. H. Kim, B. Kang, J. W. Suk, N. Li, K. S. Kim, R. S. Ruoff, W. H. Lee and K. Cho, *ACS Nano*, 2015.
25 M. Singh, M. Holzinger, M. Tabrizian, S. Winters, N. C. Berner, S. Cosnier and G. S. Duesberg, *Journal of the American Chemical Society*, 2015, **137**, 2800-2803.
26 X. Sun, Y. Mu, J. Zhang, X. Wang, P. Hu, X. Wan, Z. Guo and S. Lei, *Chemistry – An Asian Journal*, 2014, **9**, 1888-1894.
27 X. Zhang, E. H. Huisman, M. Gurram, W. R. Browne, B. J. van Wees and B. L. Feringa, *Small*, 2014, **10**, 1735-1740.
28 M. Narayanan Nair, C. Mattioli, M. Cranney, J.-P. Malval, F. Vonau, D. Aubel, J.-L. Bubendorff, A. Gourdon and L. Simon, *The Journal of Physical Chemistry C*, 2015.
29 M. Kratzer, B. C. Bayer, P. R. Kidambi, A. Matković, R. Gajić, A. Cabrero-Vilatela, R. S. Weatherup, S. Hofmann and C. Teichert, *Applied Physics Letters*, 2015, **106**, 103101.
30 S. Zhong, J. Q. Zhong, A. T. S. Wee and W. Chen, *Journal of Electron Spectroscopy and Related Phenomena*.
31 W. H. Lee, J. Park, S. H. Sim, S. Lim, K. S. Kim, B. H. Hong and K. Cho, *Journal of the American Chemical Society*, 2011, **133**, 4447-4454.
32 J. M. Englert, J. Röhrl, C. D. Schmidt, R. Graupner, M. Hundhausen, F. Hauke and A. Hirsch, *Advanced Materials*, 2009, **21**, 4265-4269.
33 C. Ehli, C. Oelsner, D. M. Guldi, A. Mateo-Alonso, M. Prato, C. Schmidt, C. Backes, F. Hauke and A. Hirsch, *Nature Chemistry*, 2009, **1**, 243-249.
34 I. Horcas, R. Fernández, J. M. Gómez-Rodríguez, J. Colchero, J. Gómez-Herrero and A. M. Baro, *Review of Scientific Instruments*, 2007, **78**, 013705.
35 B. Krajnik, T. Schulte, D. Piątkowski, N. Czechowski, E. Hofmann and S. Mackowski, *centr.eur.j.phys.*, 2011, **9**, 293-299.
36 C. D. Schmidt, C. Böttcher and A. Hirsch, *European Journal of Organic Chemistry*, 2007, **2007**, 5497-5505.
37 N. V. Kozhemyakina, J. M. Englert, G. Yang, E. Spiecker, C. D. Schmidt, F. Hauke and A. Hirsch, *Advanced Materials*, 2010, **22**, 5483-5487.
38 A. Pirkle, J. Chan, A. Venugopal, D. Hinojos, C. Magnuson, S. McDonnell, L. Colombo, E. Vogel, R. Ruoff and R. Wallace, *Applied Physics Letters*, 2011, **99**, 122108.
39 F. Taherian, V. Marcon, N. F. A. van der Vegt and F. Leroy, *Langmuir*, 2013, **29**, 1457-1465.
40 G. Hlawacek, F. S. Khokhar, R. van Gastel, B. Poelsema and C. Teichert, *Nano Letters*, 2011, **11**, 333-337.
41 C. Backes, T. Schunk, F. Hauke and A. Hirsch, *Journal of Materials Chemistry*, 2011, **21**, 3554-3557.
42 A. Kasry, A. A. Ardakani, G. S. Tulevski, B. Menges, M. Copel and L. Vyklicky, *The Journal of Physical Chemistry C*, 2012, **116**, 2858-2862.